Research Article Vol. 14, No. 12 / 1 Dec 2024 / Optical Materials Express 2982
Optical Materials EXPRESS

Recycling self-assembled colloidal quantum dot supraparticle lasers

DILLON H. DOWNIE,[1,*] CHARLOTTE J. ELING,[1] BETHAN K. CHARLTON,[1] PEDRO U. ALVES,[1] PAUL R. EDWARDS,[2] AND NICOLAS LAURAND[1]

[1]*Institute of Photonics, Department of Physics, SUPA, University of Strathclyde, Technology and Innovation Centre, 99 George Street, Glasgow G1 1RD, Scotland, UK*
[2]*Department of Physics, SUPA, University of Strathclyde, John Anderson Building, 107 Rottenrow, Glasgow G4 0 NG, Scotland, UK*
[*]*dillon.downie@strath.ac.uk*

Abstract: Supraparticles comprising semiconductor colloidal quantum dots as building blocks are a new class of microscopic lasers with a wide host of applications, including photocatalysis, biological and environmental sensing, integrated photonics, and medicine. Despite the recent advances in their fabrication, there have been no reports of their quantum dot components being recovered for use in a circular economy. Herein, we demonstrate a novel method for the recycling of these whispering-gallery-mode supraparticle lasers with a quantum dot recovery yield of 85%. The photoluminescence quantum yield of the recycled quantum dots is retained at 83 ± 16% from the initial batch of 86 ± 9%. These recycled quantum dots are then used again to synthesize distinct supraparticles via an oil-in-water emulsion self-assembly technique, allowing for the recreation of lasing supraparticles with similar thresholds to their freshly made precursors at 32.8 ± 8.2 mJ·cm^{-2} and 34.8 ± 8.6 mJ·cm^{-2}, respectively. This proof-of-concept for recyclability has the potential to complement and enhance the manufacturing of supraparticle lasers, as well as to contribute to the overall recycling efforts of a broad spectrum of colloidal nanoparticle species, aiming to improve the economic and environmental sustainability of the technology.

1. Introduction

Semiconductor colloidal quantum dots (CQDs) are finding use in many photonic applications, including color converters for solid-state lighting and display technologies, biosensing, and gain media in novel types of lasers [1]. For these applications, CQDs are either blended with other materials to form composites or assembled and densely packed together to form films or again supraparticle (SP) microspheres. These SPs are formed using a modified surfactant-stabilized directed self-assembly technique in an oil-in-water emulsion [2]. The resulting microscopic SPs have a high refractive index when compared to their surrounding medium, and due to this contrast at the interface, total internal reflection of light leads to whispering gallery modes (WGM) within the SP. This occurs on the resonance condition that the optical path length is an integer multiple of the wavelength of incident light. The SP is therefore a microresonator made of an optical gain material; the quantum dots. In turn, an individual SP can be made to lase by optical pumping [3]. Such microresonators comprised of high gain media have quality (Q) factors of ~10^3 and relatively low thresholds of approximately 100 μJ·cm^{-2} for a 100-200 fs pulse duration, but otherwise in the range of 1-100 mJ·cm^{-2} for a pump duration of 1-10 ns [4]. This is due to enhanced optical gain from quantum confinement, which allows for efficient energy transfer and stimulated emission within the resonator, paving the way for their potential as biological labels and targeted drug delivery systems [5].

#537183 https://doi.org/10.1364/OME.537183
Journal © 2024 Received 24 Jul 2024; revised 29 Oct 2024; accepted 30 Oct 2024; published 25 Nov 2024

Optical Materials EXPRESS

These SPs can be coated in protective inorganic silica or titania shells [6,7], further surface functionalized [8], embedded in flexible gels [9], or stored in water. Lasing WGMs are mostly confined to the surface boundary of a spherical resonator through total internal reflection, making them sensitive to the resonator's size and shape. Over time, however, these SPs microcavities will begin to degrade physically, resulting in a loss of a large degree of their symmetry and quality, thereby often increasing the lasing thresholds to the point where they may no longer exhibit lasing [10]. This is ultimately the unequivocal end stage for the life cycle of any given nanomaterial, particularly those exposed to oxidation by air and moisture and stored in ambient conditions. By recycling these SPs – i.e. recovering the CQDs and using them to fabricate novel SPs – we should see if their potential to lase with similar thresholds as those freshly made is retained, and in doing so increase their overall shelf life. Another significant source of overall material losses in CQD SP production is low-yielding batches, and any scalable fabrication of SP lasers would greatly benefit from the ability to reprocess defective products.

Many nanoparticle species – including CQDs – are often made from expensive, sometimes toxic, and/or scarce elements. Although the primary focus of this study is on semiconductor CQDs, there is a need for an innovative approach that can target nanoparticle aggregates on a broader scale. This is especially critical for rare-earth elements given that only 2% of them are currently recycled, with demand due to outstrip supply before the end of this decade [11]. Due to the economic viability of rare-earth recycling, studies on retrieving trace amounts from wastewater have already been conducted [12]. The recovery of rare-earth element nanoparticles from electronic waste by leveraging their electric and magnetic properties has been explored, though it requires specialized instrumentation [13], complex bio-metallurgical absorption [14], and acid leaching processes [15]. Hence, a greener technique is still sought after which can be easily paired with existing methods, such as in the separation of rare-earth species through ligand structure-selectivity [16].

The available literature on the recycling of CQD aggregates is sparse at the time of writing, alluding to the novel nature of this area. The need for CQD recycling and sustainability has, however, already been substantially addressed [17,18]. The focus now is on ensuring that the concerns of cost, hazard, and the end-of-life for these nanoparticles and their aggregates are considered before pursuing any large-scale manufacturing [19]. An ample portion of the published research highlights carbon CQDs due to their abundant and non-toxic nature, with examples emphasizing greener-synthesis strategies for creating recycled carbon CQDs from palm leaves, rice, and cellulose [20–22]. Previous studies for more toxic CQD species have focused on creating perovskite CQDs from recycled material [23], as well as the recycling and testing of similar CQDs in glass composites, demonstrating promising results with no significant reduction in photoluminescence quantum yield (PLQY) or emission properties [24]. The application of CQDs in catalysis and wastewater treatment is prevalent within scientific research [25]. Thus, this study retains relevance within these domains, especially concerning instances of nanoparticle agglomeration [26,27]. It is imperative to ensure that photocatalysts – whether they be in powder or aggregated SP form – are retrievable within aqueous environments to prevent secondary environmental pollution [28]. In studies where photocatalytic CQDs have been salvaged, their efficacy persisted over the initial 10 recycling iterations [29].

Many nanoparticle recovery processes have been prior proposed, including: filtering, scrubbing, centrifugation, flocculation/sedimentation, magnetic separation, thermal treatment, bio-metallurgical, electro-migration in solution, extraction using supercritical water [30], and selective recovery [31] to name but a few. Each, however, comes with a particular drawback such as the requirement for specific ultrafiltration centrifugation tubes in an otherwise environmentally friendly process for recycling perovskite CQDs [32]. It is important to consider what components for a recycling technique would be considered as a consumable and henceforth a black mark against the sustainable nature of the method. Furthermore, it is hoped that a method can be

Optical Materials EXPRESS

designed and tailored for laboratories that do not have access to specialist equipment, particularly in developing countries where CQDs and SPs are being considered for wastewater treatment [33]. Thus, pioneering a simple technique for recycling CQDs from SPs suspended in water ultimately takes inspiration from previous studies of microsphere controlled disassembly via ultrasonication [34–36], exploiting the low connectivity between the ligand coated CQD building blocks within the SPs in solution. This process was combined with thermal disassembly, as although CQD lasers are typically stable at varying temperatures [37], higher temperatures improve the dissolution of CQDs in organic solvents. Previous studies have shown that a temperature of 100°C is optimal for CdSe CQDs [38]. It is noted that disassembly via salt concentration and pH alteration are also avenues to consider [39]. In summary, research on the recycling of CQDs has seen notable advancement in recent years, but typically requires the CQDs to remain in their colloidal, dispersed form. Methods that have been proposed are often complex, expensive, or environmentally harmful. No studies to date have successfully recycled fully formed CQD aggregates after application such as WGM SP crystals.

In this study SPs made from the highly toxic CdS_xSe_{1-x}/ZnS oleic acid capped CQDs are recycled, and it is hoped that this method will further economize the costs already associated with direct disposal. Hence, there are both economic and environmental incentives for the recovery these materials for reuse.

There is no guarantee that SPs formed from recycled CQDs will retain their lasing properties. However, if they continue to exhibit WGM, they may still function as microresonators. In this capacity, they can still serve various applications such as in security barcoding [40], color converters, light emitting diodes, and biological sensors [41] due to their capacity for multiplexed emission spectra and often specific spectral fingerprint. As WGM SPs have the potential for further surface functionalization [8], the opportunity thus arises to recuperate these SPs after use to either re-functionalize or otherwise, with the only modifications being on the ligand exchange for the new surface functional groups of choice. In preceding research, biotin-functionalized WGM optical biosensors have been successfully regenerated via O_2 plasma treatment with no noticeable Q factor loss [42]. With these surface functionalized SPs in mind, future inquiries into incorporating this method with the recycling of the aforementioned silica- and titania-coated microspheres can be postulated through the utilization of chemical etching [43].

We address the challenges that come with the mechanical and thermal disassembly technique through the purification of the recovered CQDs followed by a ligand reattachment with surplus oleic acid to ensure all surface passive sites are re-occupied. With the operational goal to create a sustainable recycling method first and foremost, an easy, non-toxic, open-bench method was designed without the need for extreme conditions or specialized equipment. Herein, we report a facile method for reliably recycling CQDs from luminescent SPs, demonstrate that this method enables the recovery of the foundational CQDs, characterize their optical properties, and re-use them for the assembly of new SPs with the retention of lasing.

2. Experimental section

2.1. Materials

$CdSe_{1-x}S_x$/ZnS alloyed core/shell colloidal quantum dots capped with oleic acid ligands were purchased from CD Bioparticles (cat. DNP-C006) with a peak emission wavelength (λ_{em}) of 630 nm in toluene. Poly(vinyl alcohol) (PVA) 87–89 kDa, Rhodamine B ($\lambda_{em} = 575$ nm in ethanol), ethanol 99%, toluene 99%, hexane 99%, oleic acid, hydrochloric acid (HCl) 37%, sodium hydroxide (NaOH) 25 mM solution, and chloroform 99% were purchased from Merck. Water was purified with a Milli-Q water purification system (Milli-Q IQ 7000, Ultrapure Lab Water System, Merck Millipore).

Optical Materials EXPRESS

2.2. Supraparticle fabrication

The fabrication of SPs between 1 and 20 μm in diameter by the assembly of alloyed core-shell $CdSe_{1-x}S_x$/ZnS CQDs with a nominal size 5.5 - 6.5 nm through an oil-and-water emulsion was performed as illustrated by steps 1–3 in Fig. 1. Here, a 1.25% by weight solution of PVA in distilled Milli-Q water was mixed with the CQDs suspended in chloroform by way of vortexing (VWR Advanced Heavy-Duty Vortex Mixer) at 2000rpm for 10 seconds and followed by ultrasonication (Bandelin Sonorex Super RK31) operating at 35 kHz for 10 seconds. The two immiscible liquids were then further stirred for 2 hours at 350 rpm at room temperature until the chloroform had completely evaporated.

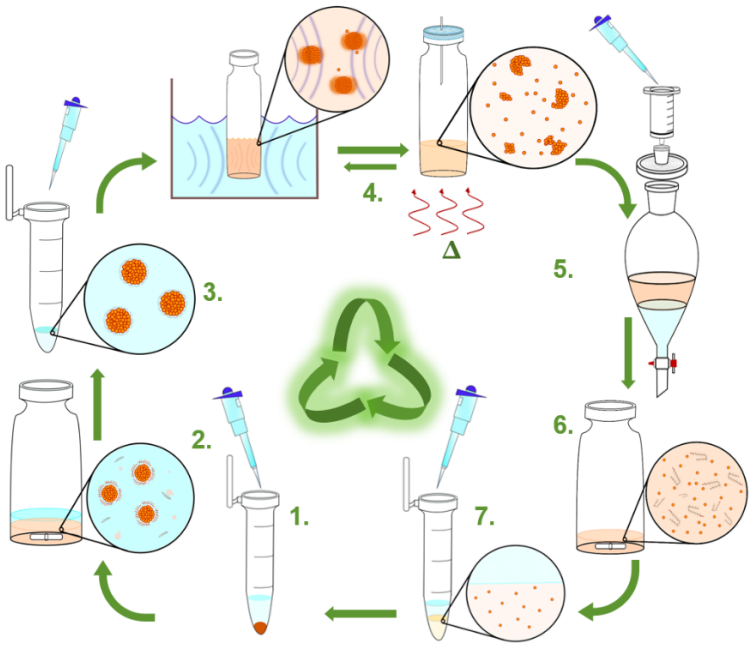

Fig. 1. The unified process of SP fabrication and recycling; 1. CQD precipitation, 2. Self-assembly, 3. Completed fabrication of SPs, 4. Sonication & heat treatments, 5. Separation & filtration, 6. Ligand re-attachment, 7. Recovery of CQDs.

2.3. Colloidal quantum dot recycling

This process required all equipment used to be devoid of contaminants at every stage obtained through thorough washings with methanol, toluene, and acetone, followed by pneumatic cleansing with pressurized gas – which in this instance was nitrogen – in a fume hood to ensure its cleanliness prior to use. This was to limit the potential for nucleation sites around which the CQDs can aggregate. Additionally, this is to maintain a high level of purity which will show up later in the quality of the reformed supraparticles.

After optical characterization, a portion of the SP sample was taken and recycled as illustrated by steps 4–7 in Fig. 1. The SPs were disassembled in toluene via repeated ultrasonic and high temperature cycles. The ultrasonication operated at 35 kHz for 2 hours at room temperature, followed by the heat treatments of 105°C for 2 hours on a hotplate. This was followed by filtration with 0.2 μm pore size cellulose syringe filters (Whatman) and a water-oil phase separation purification process with a separatory funnel to facilitate the removal of excess PVA surfactant and any other water-soluble impurities. A modified ligand exchange reaction was carried out

Optical Materials EXPRESS

using excess oleic acid in hexane for the purpose of ensuring ligand re-attachment had been successful. This is to ensure ligand saturation in any vacant active sites on the surface of the CQDs that could arise as a consequence of the heating and ultrasonication cycles. The CQDs thus recuperated were then re-used to synthesize new SPs following the same method of fabrication as prior. The yield for the recycling process was calculated as follows:

$$yield(\%) = \left(\frac{mass\ of\ recycled\ CQDs}{mass\ of\ initial\ CQDs}\right) \cdot 100 \quad (1)$$

Here, the mass of the initial CQDs was taken as the mass of CQDs used to make the initial SP sample, and the mass of recycled CQDs was taken as the mass of recycled CQDs prior to the refabrication of SPs.

2.4. Optical characterization

Absorption and photoluminescence (PL) spectra of the recycled CQDs were measured as well as their PLQY. The optical emission of the SPs made from recycled CQDs under nanosecond pulse optical pumping were compared to that of the original SPs. For the optical emission of individual SPs under pulse operation, a sample of SPs at a ratio of 1:50 by volume in water were dropcast onto a glass slide and left to dry. Subsequently, an SP was found and optically pumped on a micro-photoluminescence (μPL) setup illustrated in Fig. S1, using a 5 ns pulsed Nd:YAG laser ($\lambda = 355$ nm) at a repetition rate of 10 kHz and a beam spot radius of $1.54 \times 10^{-5} \pm 0.21 \times 10^{-5}$ cm^2. A spectrometer (AvaSpec-2048-4-DT with a spectral resolution of 0.6 nm between 200-1100 nm, Avantes) was used for spectral data acquisition. All spectra were an average of five separate two second recordings under excitation. SP sizes were measured using ImageJ 1.53 t software with images taken from an optical microscope equipped with a CCD camera (DCC1645C, Thorlabs) and a digital scale bar for reference (see Visualization 1). Individual lasing SPs were found by initially detecting strong PL with the μPL spectrometer, followed by using the CCD camera to capture the SP for size measurement in conjunction with the ImageJ software. Errors in SP sizes were calculated using the pixel resolution at a given scale around the defined borders between the background and SP edge. Scanning electron microscopy (SEM) was carried out using the JEOL JSM-IT100 InTouchScope to study the surface morphology and size distribution of the SPs, operating at 20 kV at probe current 30-60 under high vacuum at a working distance of 10 mm. PLQY values were obtained via the comparative method with an aqueous solution of Rhodamine B as the standard. Absorption spectra were measured both using a Genesys 30 UV-visible absorbance spectrometer (Thermo Fisher Scientific Inc.) and a Cary 60 UV-vis spectrophotometer (Agilent Technologies Inc.). The PL spectra of the CQDs suspended in toluene was recorded using a continuous-wave, 10 mW, 532 nm laser (DJ532-10, Thorlabs) for excitation, and a fiber-coupled OceanOptics USB4000 spectrometer (Ocean Insight) for detection. For the measurement of the CQDs' zeta potential, a Zetasizer Nano ZS series (Malvern Panalytical Ltd) was used with 1 ml disposable plastic cuvette, a Universal Malvern Dip Cell, and all CQDs measured in hexane. The pH was adjusted by adding 2 µL aliquots of NaOH or HCl (1 mM in water) and measured using the Jenway 3510 benchtop pH meter.

3. Results and discussion

3.1. Viability of colloidal quantum dot recycling

The calculated yield for the optimized recycling process and recovery of CQDs was found to be 85%. The size distributions for both the original and recycled SPs found in Fig. 2 provided an average SP diameter of 2.7 ± 1.6 µm and 4.0 ± 2.9 µm with the extrapolated polydispersities of approximately 58% and 74%, respectively. These values were found using the ImageJ size analysis of SEM images provided in Fig. S2. The disparity between the mean radii is a result of

Optical Materials EXPRESS

the emulsion method used in the SP fabrication, as experimental conditions such as temperature, pH, and electrostatic charges in the laboratory often vary.

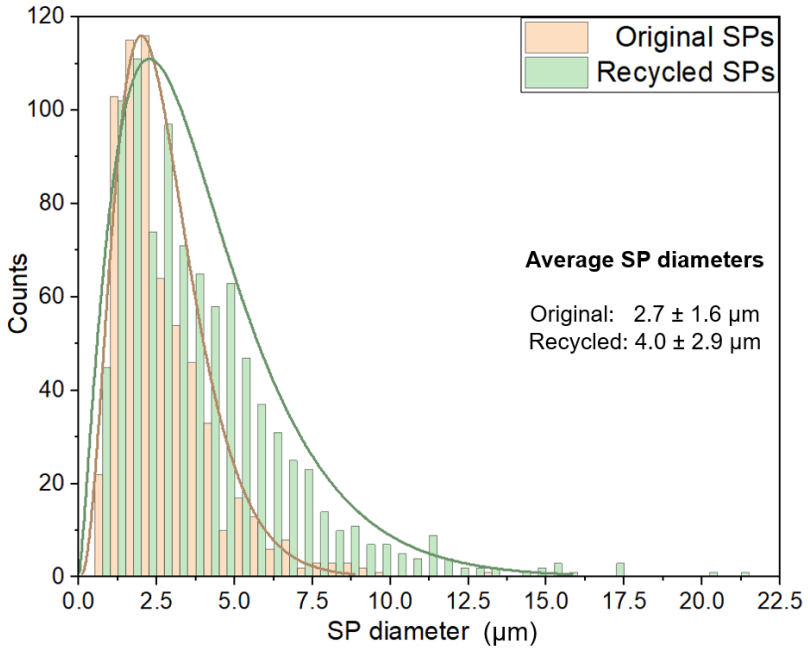

Fig. 2. The size dispersions for both the initially fabricated SPs and the SPs fabricated from the CQDs recycled from the original batch, along with their corresponding mean diameters.

During the recycling process, the SPs are broken down back to individual CQDs. Throughout this process, some surface ligands may be removed due to intense sonication and heat cycles. This can affect the solubility and PLQY of the CQDs. The recycled CQDs were therefore mixed with oleic acid, to ensure that the surface was saturated with the capping ligand. The zeta (ζ) potential is a measure of the surface charge at the surface of the CQD in a colloidal dispersion, which can determine a sample's proclivity to coagulate and therefore its overall stability in suspension. For CQDs, this charge is highly dependent on the presence of ligand binding at the surface, and so the technique can be implemented to measure changes in the ligands present [44]. The surface modification by ligand reattachment was confirmed through zeta potential measurements, which demonstrated a change in the surface charge at a pH of 6.5. Before any SP fabrication, CQD recycling, or ligand modification, the CQDs exhibited a surface charge of -13.8 ± 9.48 mV. Prior to ligand reattachment, the recycled CQDs exhibited an increased surface charge of 17.6 ± 20.8 mV, while post-ligand reattachment, this value reduced to 4.44 ± 9.87 mV. This decrease in zeta potential for the CQDs after ligand reattachment aligned with the expectation for a return towards a negative value, as can be found in the literature [45,46]. The errors in these values represent the variability within their respective distributions, visualized in Figs. S3, S4 and S5. The higher, positive zeta potential value for the recycled CQDs pre-ligand reattachment, which is consistent with the literature values for uncoated CQDs [47], contributes evidence towards an observed loss of ligand coating.

Assuming, therefore, that there has been ligand loss, it is crucial to recoat the CQDs with ligands to prevent future aggregation [48], thus extending their service life. In the initial recycling experiments without the addition of oleic acid ligands, the SPs fabricated were notably less spherical as shown in Fig. S6, and did not retain the ability to lase upon excitation via the μPL setup despite exhibiting WGM resonance depicted in Fig. S7. This can be partially explained

Optical Materials EXPRESS

by the loss of surface ligands on the CQDs which will affect the attractive Van der Waals and repulsive steric forces involved with inter-particle aggregation during the self-assembly process. Here, an insufficient amount of oleic acid ligand lowers the surface free energy for each CQD, resulting in the incomplete aggregation of CQDs into non-spherical SPs [49]. This appears to have been remedied with the inclusion of a ligand reattachment step and the consequent re-emergence of spherical SP microlasers. To measure the efficiency as a ratio of photons absorbed vs photons emitted, PLQY measurements were carried out using a fluorimetric method [50]. The PLQY for the CQDs before and after recycling was extracted from a linear regression plot of the absorption and PL spectra over a range of known CQD concentrations in toluene against the standard Rhodamine B of a known PLQY of 31%, shown in Fig. S8. The calculated values for the recycled CQDs were determined to be $83 \pm 16\%$ down from the $86 \pm 9\%$ characteristic of the original CQDs. The retention of a high PLQY similar to the original CQDs suggests no significant increase in the rate of non-radiative processes, insofar that the CQDs maintain sufficient efficiency as to act as gain material in refabricated SP lasers.

3.2. Supraparticle analysis

An SP from the original fresh batch was fully characterized and compared to an SP from the recycled batch, as seen in Fig. 3. To find the laser transfer functions for the SPs, the peak spectral emission intensity over increasing pump fluences were integrated over the spectral range of the dominant lasing peaks at 636 nm for the original SP, and 631 nm for the recycled SP. The two peaks seen in both SPs correspond to two different lasing modes within the same SP. While each SP may support several closely spaced WGMs, different WGMs may oscillate (lase) depending on the size of the SP. Figure 4 of the resulting transfer function displays the transition slopes for spontaneous emission and laser oscillation of each SP. From this, the laser thresholds are found as the fluence at the point where the two slopes intersect. For the original SP (11.5 ± 0.5 µm) and recycled SP (5.5 ± 0.5 µm) the laser thresholds were found to be 32.8 ± 8.2 mJ·cm^{-2} and 34.8 ± 8.6 mJ·cm^{-2}, as indicated. Alongside the similar thresholds, the conversion efficiencies above threshold was calculated using the following equation, which defines the slope above threshold:

$$Conversion\ efficiency = \frac{\Delta integrated\ emission}{\Delta fluence} \tag{2}$$

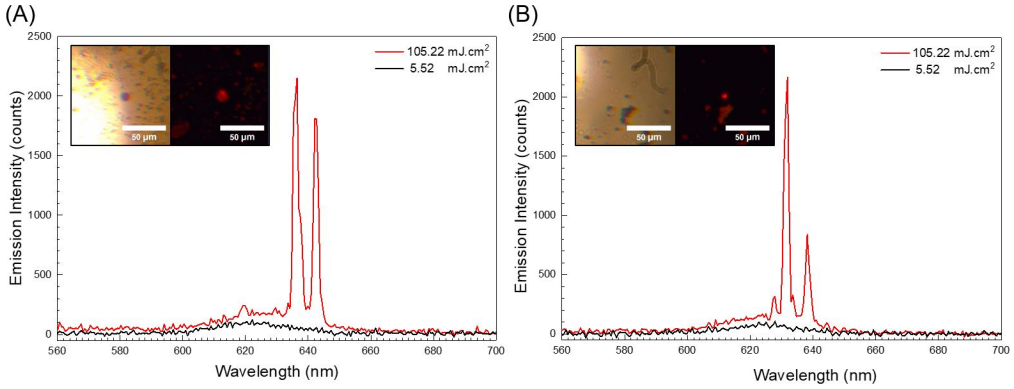

Fig. 3. PL spectra for the (A) SP from the original batch (diameter of 11.5 ± 0.5 µm) and (B) SP from the recycled batch (5.5 ± 0.5 µm). Each graph displays clear distinction between emission spectra for both below (black) and above (red) lasing threshold. The inset of each PL spectrum contains an image of the corresponding SP under lamp illumination (left) and above lasing threshold (right). The scale bar is 50 microns.

Optical Materials EXPRESS

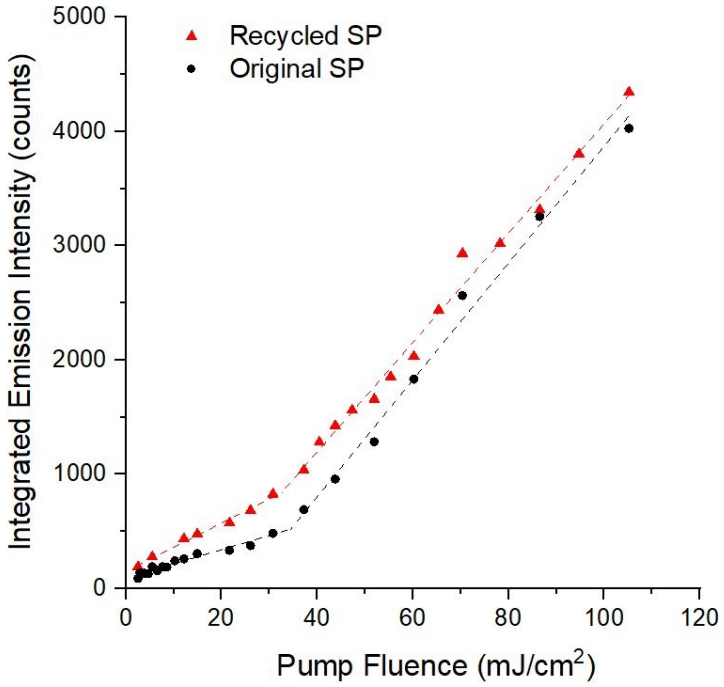

Fig. 4. The laser transfer function for the dominant lasing WGM peaks of both an original SP (11.5 ± 0.5 μm) and a recycled SP (5.5 ± 0.5 μm).

The resultant conversion efficiencies are also similar at 51 ± 2 and 48 ± 2 counts/mJ·cm^{-2}. Despite the recycled SP being approximately half the diameter of the original SP, it demonstrates a higher intensity of emission. We hypothesize that, as a result of the recycling process, there is a greater packing density of fluorescent material. This could be attributed to the recycling process, which leaves the CQDs with less ligand cover. Consequently, they are able to aggregate more tightly, leading to a higher gain per unit of volume.

Given the size of our SPs, WGMs that oscillate are mostly confined to the surface boundary and are dependent on the sphere's geometry and the refractive index contrast between the sphere and its surroundings. For an individual SP, this is the radius (R) and the effective refractive index (n_{eff}), with the one path of light around the equator for a WGM approximated to $2\pi R$. As spherical microresonators, WGMs occur in multiple dimensions (polar, radial, and azimuthal), and thus have, for each polarization, associated angular components with quantum numbers (n, l, and m) [51]. The spherical harmonic nature of these WGM SPs ensures that only certain discrete wavelengths (λ) are supported, from which the pseudo-free spectral range (FSR) – or the wavelength spacing between successive angular mode numbers – can be approximated. By taking the peak wavelength value obtained from the PL spectra, the FSR can be calculated to find an estimated value for this wavelength separation ($\Delta\lambda$) between consecutive WGMs [52]. Here, the n_{eff} value was taken as 1.7 [53].

$$FSR = \Delta\lambda \approx \frac{\lambda^2}{2\pi n_{eff} R} \tag{3}$$

The spectral data was filtered by calculating the moving average at the expected FSR and removing the main PL emission using Wolfram Mathematica. A discrete Fourier transform (DFT) was performed to find probable FSR values as depicted in Fig. 5. The closest peak to the estimated pseudo-FSR value was then taken as the actual FSR value, which for the original

Optical Materials EXPRESS

and recycled SPs was 6.4 and 10.6 ± 0.6 nm, correspondingly. Note that from the actual FSR values, this equation can provide approximate n_{eff} values of 1.7 and 2.0. This increased n_{eff} for the recycled SP could account for the increased brightness of the recycled SP relative to the larger SP from the initial batch, supporting the hypothesis of a higher density of CQD gain material per unit of volume in the recycled sphere.

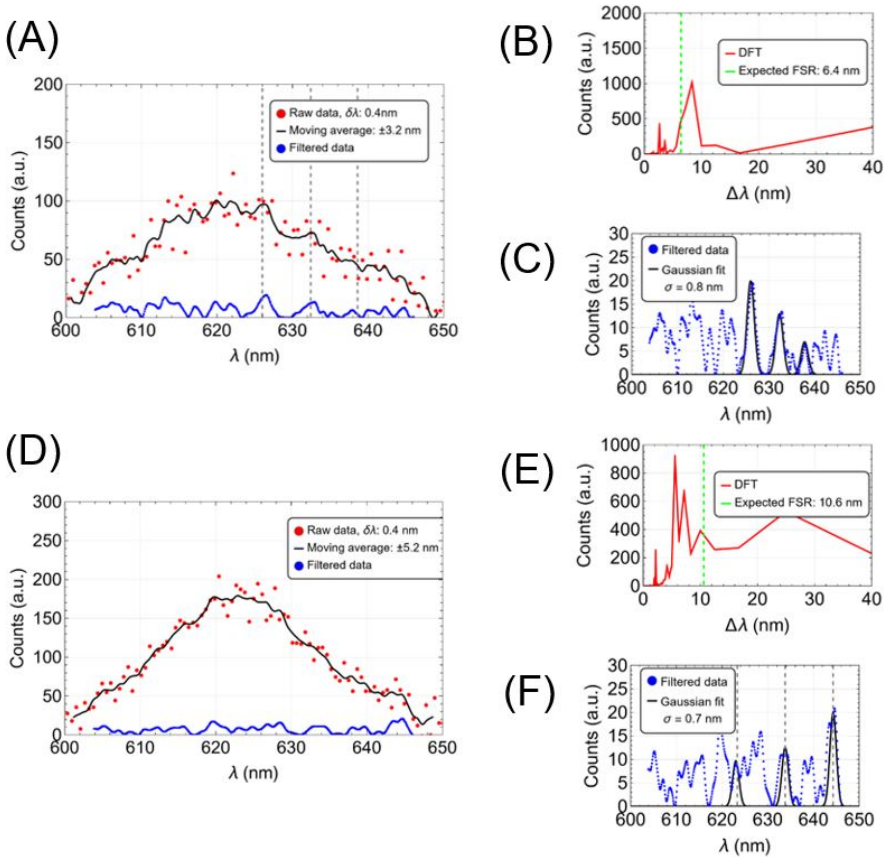

Fig. 5. The raw and filtered WGM PL spectra below threshold (A), the DFT (B), and the Gaussian operation (C) for an original SP (11.5 ± 0.5 μm). The raw and filtered WGM PL spectra below threshold (D), the DFT (E), and the Gaussian operation (F) for a recycled SP (5.5 ± 0.5 μm).

Once the FSR is known, it's easier to spot the modes in the PL (Fig. 5(A) and Fig. 5(D)). These modes were analyzed individually by fitting each one of them to a Gaussian (Fig. 5(C) and Fig. 5(F)). The Q factor, defined as a WGM resonators ability to store energy at a given frequency [54], was calculated for each individually pumped original and recycled SPs near the 630 nm WGM wavelength position using the following equation:

$$Q = \frac{\lambda}{\Delta\lambda} \tag{4}$$

where $\Delta\lambda$ is the full width at half maximum (FWHM) at wavelength λ of that particular lasing peak WGM, found by taking a Gaussian fit of the peak below threshold in Fig. 5. From this we calculate approximate values for the Q factors as 340 ± 70 for the original SP and 380 ± 40 for the recycled SP.

Optical Materials EXPRESS

As the pump energy increases, one or several of these modes will go past the lasing threshold resulting in the pronounced and narrow peaks seen in Fig. 3 (both for the original and recycled SPs). The lasing peaks can be separated into a range of different modes accounted for by the phenomenon of selective mode enhancement, deriving from mode competition processes such as spatial hole burning [55].

To summarize, from the lasing threshold and PL spectral data there does not appear to be a meaningful difference in overall CQD and SP quality, to the extent that they continue to lase. The apparent disparity in the average sizes of lasing SPs fabricated between the original and recycled batches can be attributed to variations inherent in the self-assembly fabrication reaction procedure itself, a factor that has been observed in the literature when employing this technique [4,8]. Other noticeable discrepancies in the microsphere morphology can be seen in Fig. 6, with a higher degree of surface microporosity seen in the original SPs than in the recycled SPs. This can be rationalized not by the CQDs present but through the reaction conditions that direct the fabrication, such as humidity, temperature, and the surfactant and solvent types [56,57]. A higher porosity and subsequent lower density would corroborate the apparent disparity in n_{eff} values and Q factors. While solvent and surfactant choice is a key component for the quality and reproducibility of SP synthesis, this method was chosen for its simplicity where only PVA was used as the emulsion stabilizing surfactant. Additional research on the solvent and surfactant species of choice is warranted to investigate the effect on the recycling viability.

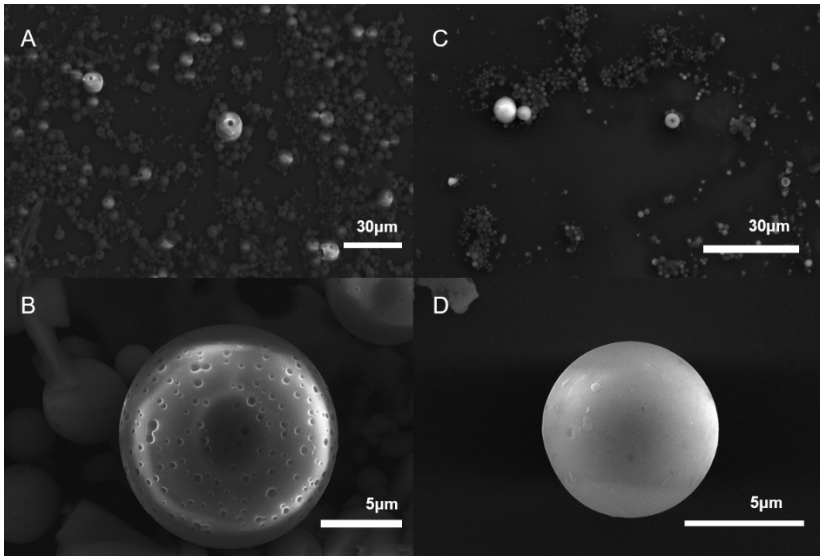

Fig. 6. SEM images of (A) the original batch of SPs, (B) an individual SP from the original batch, (C) the recycled batch of SPs, and (D) an individual SP from the recycled batch. The scale bars range between 5 and 30 microns, but do not share uniform length.

While there is no discernible change evident in the Stokes shift in either the absorption or PL spectra between the original and recycled CQDs as displayed in Fig. S9, the spectra above threshold reveals the emergence of a laser peak shifting phenomenon for the recycled SP as the pump energy is increased. Here, in the recycled SPs that were formed and exhibited dominant WGM lasing peaks, the dominant WGM lasing peak maxima blue shifts by 2 - 4 ± 0.6 nm as seen in Fig. S10.

One tentative explanation could be photodegradation. Oxidation upon exposure to environmental oxidizers before, during, or after the recycling process such as in the presence of moisture and air, as has been seen prior in cadmium CQDs and silicon QD aggregates [58,59]. However,

Optical Materials EXPRESS

as the blue-shift arises at high fluences, photophysical degradation and the subsequent loss of surface ligand, restructuring of the surface atomic structure, and photo-oxidation has been suggested as a cause for the increase of surface trap states [60]. As these trap states arise, the size of the SP CQDs may decrease through photobleaching and thermally assisted quenching, resulting in a possible n_{eff} decrease and subsequent blue-shift. As quantum wells, the CQD band structure will be sensitive to the modification of even just the surface layer induced by oxidation. It is reasonable to assume that even if only the top layer is partially oxidized while other layers underneath remain intact, a potential barrier for carriers will form between the top layer and the rest of the sample [61].

This blue-shifting has not been observed in the original SPs above threshold. Therefore, further analysis is essential to determine if the blue-shifting is a result of a permanent photoactivated change resulting in an altered n_{eff}, or if it redshifts back to sub-threshold positions. Currently, it remains to be seen whether this loss in surface stability is a direct result of the recycling process, deficiencies with the recuperated CQD surfaces, or an entirely separate phenomenon.

4. Conclusion

In summary, we have developed an inexpensive, facile, and resource-efficient method to retrieve CQDs from SP lasers. Novel SPs can be formed with the recovered CQDs while retaining WGM lasing characteristics for repurposed photonic applications and greater sustainability. The method demonstrates excellent practicality without the need for specialist equipment, ultrahigh pressures/temperatures, or extensive in-house synthesis. This study provides a proof-of-concept for recyclable SP CQD lasers with analogous Q factors, PLQY values, and lasing thresholds to their parent materials. Accordingly, this method unlocks the potential for continued investigation into the recycling of other nanoparticle species, crucially rare-earth up-converting nanoparticles, and is expected to be fully scalable. Follow-up studies are required to ascertain the durability of such nanoparticles over multiple recycles, with a focus on their continued ability to exhibit lasing emission. With further modification, this approach shows promise for the recycling of more complex functionalized, capped, or otherwise encapsulated SP species.

Funding. Leverhulme Trust (RL-2019-038).

Acknowledgements. We would like to thank Dr Sian Sloan-Dennison and Benjamin Clark for access to and the training of the Zetasizer and Cary 60 UV-visible Spectrophotometer, and Dr Natalie Bruce for training on the method for PLQY measurement acquisition. **Author contributions.** D.H.D., C.J.E., and N.L. conceived of the idea and designed the experiments. D.H.D. performed the experiments and obtained the SEM data. C.J.E. aided with acquiring the PLQY and μPL data. P.U.A analyzed the data and performed DFT and Q factor calculations, B.K.C provided analysis for the zeta potential and threshold data, P.R.E. provided training for and access to the SEM. D.H.D. wrote the original paper and C.J.E, P.U.A., B.K.C., P.R.E., and N.L. reviewed and edited the manuscript.

Disclosures. The authors declare no conflicts of interest.

Data Availability. Data underlying the results presented in this paper are available from the University of Strathclyde data repository [62] or from the corresponding author upon reasonable request.

Supplemental document. See Supplement 1 for supporting content.

References

1. V. I. Klimov, A. A. Mikhailovsky, S. Xu, *et al.*, "Optical gain and stimulated emission in nanocrystal quantum dots," Science **290**(5490), 314–317 (2000).
2. F. Montanarella, D. Urbonas, L. Chadwick, *et al.*, "Lasing supraparticles self-assembled from nanocrystals," ACS Nano **12**(12), 12788–12794 (2018).
3. M. Humar and S. H. Yun, "Intracellular microlasers," Nat. Photonics **9**(9), 572–576 (2015).
4. P. U. Alves, B. J. E. Guilhabert, J. R. McPhillimy, *et al.*, "Waveguide-integrated colloidal nanocrystal supraparticle lasers," ACS Appl. Opt. Mater. **1**(11), 1836–1846 (2023).
5. V. Blondot, A. Bogicevic, A. Coste, *et al.*, "Fluorescence properties of self assembled colloidal supraparticles from CdSe/CdS/ZnS nanocrystals," New J. Phys. **22**(11), 113026 (2020).
6. C. J. Eling, N. Laurand, N. Gunasekar, *et al.*, "Silica coated colloidal semiconductor quantum dot supracrystal microlasers," in *2022 IEEE Photonics Conference (IPC)* (2022), pp. 1–2.

Optical Materials EXPRESS

7. C. J. Eling and N. Laurand, "Photocatalytic-ready supraparticle lasers," in *2023 IEEE Photonics Conference (IPC)* (2023), pp. 1–2.
8. B. K. Charlton, D. H. Downie, I. Noman, *et al.*, "Surface functionalisation of self-assembled quantum dot microlasers with a DNA aptamer," Int. J. Mol. Sci. **24**(19), 14416–14428 (2023).
9. L. Gonçalves, P. Lavrador, A. J. R. Amaral, *et al.*, "Double-interlinked colloidal gels for programable fabrication of supraparticle architectures," Adv. Funct. Mater. **33**(2304628), 1–14 (2023).
10. S. J. Neuhaus, E. Marino, C. B. Murray, *et al.*, "Frequency stabilization and optically tunable lasing in colloidal quantum dot superparticles," Nano Lett. **23**(2), 645–651 (2023).
11. V. S. Efstratiadis and N. Michailidis, "Sustainable recovery, recycle of critical metals and rare earth elements from waste electric and electronic equipment (circuits, solar, wind) and their reusability in additive manufacturing applications: a review," Metals **12**(5), 794 (2022).
12. C. Li, Z. Zhuang, F. Huang, *et al.*, "Recycling rare earth elements from industrial wastewater with flowerlike nano-$Mg(OH)_2$," ACS Appl. Mater. Interfaces **5**(19), 9719–9725 (2013).
13. T. G. Ambaye, M. Vaccari, F. D. Castro, *et al.*, "Emerging technologies for the recovery of rare earth element (REEs) from the end-of-life electronic wastes: a review on progress, challenges, and perspectives," Environ. Sci. Pollut. Res. **27**(29), 36052–36074 (2020).
14. T. Xu, X. Zheng, B. Ji, *et al.*, "Green recovery of rare earth elements under sustainability and low carbon: a review of current challenges and opportunities," Sep. Purif. Technol. **330**(125501), 125501 (2024).
15. O. Artiushenko, W. S. Rojano, M. Nazarkovsky, *et al.*, "Recovery of rare earth elements from waste phosphors using phosphonic acid-functionalized silica adsorbent," Sep. Purif. Technol. **330**(125525), 125525 (2024).
16. L. Li, X. Hu, Z. Wang, *et al.*, "Structure-activity relationship approach toward the improved separation of actinides(III) over lanthanides(III) using amine-triamide ligands," Sep. Purif. Technol. **330**(125545), 125545 (2024).
17. N. T. Kalyani, H. Nagabhushana, M. Michalska-Domańska, *et al.*, "Sustainability, recycling, and lifetime issues of quantum dots," in *Quantum Dots: Emerging Materials for Versatile Applications* (Elsevier, 2023), pp. 575–580.
18. S. Wintzheimer, J. Reichstein, P. Groppe, *et al.*, "Supraparticles for sustainability," Adv. Funct. Mater. **31**(2011089), 1–31 (2021).
19. S. Wickerts, R. Arvidsson, B. A. Sandén, *et al.*, "Prospective life-cycle modeling of quantum dot nanoparticles for use in photon upconversion devices," ACS Sustainable Chem. Eng. **9**(14), 5187–5195 (2021).
20. H. Saleem, A. Saud, and S. J. Zaidi, "Sustainable preparation of graphene quantum dots from leaves of date palm tree," ACS Omega **8**(31), 28098–28108 (2023).
21. M. Kumari, G. R. Chaudhary, S. Chaudhary, *et al.*, "Transformation of waste rice straw to carbon quantum dots and their potential chemical sensing application: green and sustainable approach to overcome stubble burning issues," Biomass Conv. Bioref. **14**(6), 7507–7518 (2024).
22. W. Zou, Z. Ma, and P. Zheng, "Preparation and functional study of cellulose/carbon quantum dot composites," Cellulose **27**(4), 2099–2113 (2020).
23. L. Chen, C. Tien, S. Ou, *et al.*, "Perovskite $CsPbBr_3$ quantum dots prepared using discarded lead-acid battery recycled waste," Energies **12**(6), 1117 (2019).
24. N. Vahedigharehchopogh, E. Erol, O. Kıbrıslı, *et al.*, "Recyclability of $CsPbBr_3$ quantum dot glass nanocomposites for their long-standing use in white LEDs," J. Mater. Chem. C **10**(42), 16088–16099 (2022).
25. Q. Liu, M. Zhang, Y. Han, *et al.*, "Recyclable copper indium sulfide quantum dots for photocatalytic homocoupling of arenediazonium tetrafluoroborates," ACS Sustainable Chem. Eng. **11**(50), 17697–17707 (2023).
26. H. K. Melvin Ng and C. P. Leo, "The coherence between TiO_2 nanoparticles and microfibrillated cellulose in thin film for enhanced dispersal and photodegradation of dye," Prog. Org. Coat. **132**, 70–75 (2019).
27. H. Shen, W. Zhang, C. Guo, *et al.*, "Natural cotton cellulose-supported TiO_2 quantum dots for the highly efficient photocatalytic degradation of dyes," Nanomaterials **12**(18), 3130 (2022).
28. W. Zu, G. Bai, E. Pan, *et al.*, "Advances, optical and electronic applications of functional materials based on rare earth sulphide semiconductors," Mater. Des. **238**(112698), 112698 (2024).
29. W. A. A. Mohamed, H. H. Abd El-Gawad, H. A. Mousa, *et al.*, "Photophysical properties, antimicrobial activity, energy consumption and financial cost of recycling of TiO_2 quantum dots via photomineralization processes of vat green dye and industrial dyeing effluents," Ceram. Int. **50**(9), 15312–15324 (2024).
30. F. Xiu and F. Zhang, "Size-controlled preparation of Cu_2O nanoparticles from waste printed circuit boards by supercritical water combined with electrokinetic process," J. Hazard. Mater. **233-234**, 200–206 (2012).
31. H. Gavilán, M. B. Serrano, and J. C. Cabanelas, "Nanomaterials and their synthesis for a sustainable future," in *New materials for a Circular Economy* (Materials Research Forum LLC, 2023), vol. 149, pp. 233–310.
32. J. Chen, Y. Kong, S. Feng, *et al.*, "Recycled synthesis of whey-protein-capped lead sulfide quantum dots as the second near-infrared reporter for bioimaging Application," ACS Sustainable Chem. Eng. **4**(6), 2932–2938 (2016).
33. K. Hou, J. Han, and Z. Tang, "Formation of supraparticles and their application in catalysis," ACS Mater. Lett. **2**(1), 95–106 (2020).
34. L. Moreau, F. Ziarelli, M. W. Grinstaff, *et al.*, "Self-assembled microspheres from f-block elements and nucleoamphiphiles," Chem. Commun. **1**(15), 1661–1663 (2006).
35. Y. Wang, H. Arandiyan, H. A. Tahini, *et al.*, "The controlled disassembly of metostructured perovskites as an avenue to fabricating high performance nanohybrid catalysts," Nat. Commun. **8**(1), 15553 (2017).

Optical Materials EXPRESS

36. L. Zhou, K. Zu, H. Zhu, *et al.*, "Magnetic microsphere with hierarchical LDH/polydopamine shell encapsulated Fe_3O_4 core for carrying Ag nanocatalyst," Colloids Surf., A **601**(25022), 125022 (2020).
37. Y. Zhi and A. Meldrum, "Tuning a microsphere whispering-gallery-mode sensor for extreme thermal stability," Appl. Phys. Lett. **105**(3), 1–5 (2014).
38. J. T. Siy and M. H. Bartl, "Insights into reversible dissolution of colloidal CdSe nanocrystal quantum dots," Chem. Mater. **22**(21), 5973–5982 (2010).
39. N. Morimoto, K. Muramatsu, T. Wazawa, *et al.*, "Self-assembled microspheres driven by dipole-dipole interactions: UCST-type transition in water," Macromol. Rapid Commun. **35**(1), 103–108 (2014).
40. B. Xu, S. Yang, X. Feng, *et al.*, "Dual-stimuli responsive photonic barcodes based on perovskite quantum dots encapsulated in whispering-gallery-mode microspheres," J. Materiomics **9**(3), 423–430 (2023).
41. A. Khan, P. Ezati, J. T. Kim, *et al.*, "Biocompatible quantum dots for intelligent sensing in food safety applications: opportunities and sustainability," Mater. Today Sustain. **21**(00306), 100306 (2023).
42. H. K. Hunt and A. M. Armani, "Recycling microcavity optical biosensors," Opt. Lett. **36**(7), 1092–1094 (2011).
43. T. Kondratowicz, S. Slang, L. Dubnová, *et al.*, "Controlled silica core removal from SiO_2@MgAl core-shell system as a tool to prepare well-oriented and highly active catalysts," Appl. Clay Sci. **216**(06365), 106365 (2022).
44. J. Sanmartín-Matalobos, P. Bermejo-Barrera, M. Aboal-Somoza, *et al.*, "Semiconductor quantum dots as target analytes: properties, surface chemistry and detection," Nanomaterials **12**(14), 2501 (2022).
45. J. Kim, D. W. Hwang, H. S. Jung, *et al.*, "High-quantum yield alloy-typed core/shell CdSeZnS/ZnS quantum dots for bio-applications," J. Nanobiotechnol. **20**(1), 22 (2022).
46. J. An, K. H. Huynh, Y. Ha, *et al.*, "Surface modification of a stable CdSeZnS/ZnS alloy quantum dot for immunoassay," J. Nanomater. **2020**(4937049), 1–9 (2020).
47. M. V. Reymatias, A. Senthil, D. Bosomtwi, *et al.*, "Synthesis and characterization of colloidal $CdSe_xS_{1-x}$/ZnS quantum dots," Proc. SPIE **11255**, 5–12 (2020).
48. S. K. E. Hill, R. Connell, C. Peterson, *et al.*, "Silicon quantum dot-poly(methyl methacrylate) nanocomposites with reduced light scattering for luminescent solar concentrators," ACS Photonics **6**(1), 170–180 (2019).
49. G. Yang, H. Zhong, R. Liu, *et al.*, "In situ aggregation of ZnSe nanoparticles into supraparticles: shape control and doping effects," Langmuir **29**(6), 1970–1976 (2013).
50. T. Aaboub, A. Boukhriss, S. Gmouh, *et al.*, "Determination of photoluminescence quantum yields in dilute solution using non-monochromatic excitation light," Photochem. Photobiol. Sci. **22**, 465–475 (2022).
51. T. J. A. Kippenberg, "Nonlinear optics in ultra-high-Q whispering gallery optical microcavities," *Doctoral dissertation*, California Institute of Technology (2004).
52. G. C. Righini, Y. Dumeige, P. Féron, *et al.*, "Whispering gallery mode microresonators: fundamentals and applications," Riv. Nuovo Cim. **34**(7), 435–488 (2011).
53. L. J. McLellan, B. J. E. Guilhabert, N. Laurand, *et al.*, "CdS_xSe_{1-x}/ZnS semiconductor nanocrystal laser with sub 10 kW/cm^2 threshold and 40nJ emission output at 600 nm," Opt. Express **24**(2), A146–153 (2016).
54. Y. Zheng, Z. Wu, P. P. Shum, *et al.*, "Sensing and lasing applications of whispering gallery mode microresonators," Opto-Electron. Adv. **1**(9), 18001501 (2018).
55. Y. Liang, H. Zhu, H. Zheng, *et al.*, "Competition of whispering gallery lasing modes in microwire with hexagonal cavity," J. Phys. D: Appl. Phys. **54**(5), 055107 (2021).
56. W. Liu, M. Kappl, and J. H. Butt, "Tuning the porosity of supraparticles," ACS Nano **13**(12), 13949–13956 (2019).
57. A. Plunkett, C. Eldridge, G. A. Schneider, *et al.*, "Controlling the large-scale fabrication of supraparticles," J. Phys. Chem. B **124**(49), 11263–11272 (2020).
58. K. Pechstedt, T. Whittle, J. Baumberg, *et al.*, "Photoluminescence of colloidal CdSe/ZnS quantum dots: the critical effect of water molecules," J. Phys. Chem. C **114**(28), 12069–12077 (2010).
59. X. Pi, T. Yu, and D. Yang, "Water-dispersible silicon-quantum-dot-containing micelles self-assembled from an amphiphilic polymer," Part. & Part. Syst. Charact. **31**(7), 751–756 (2014).
60. N. J. Orfield, S. Majumder, J. R. McBride, *et al.*, "Photophysics of thermally-assisted photobleaching in "giant" quantum dots revealed in single nanocrystals," ACS Nano **12**(5), 4206–4217 (2018).
61. F. Wang, G. Zhang, S. Huang, *et al.*, "Electronic structures of air-exposed few-layer black phosphorus by optical spectroscopy," Phys. Rev. B **99**(7), 075427 (2019).
62. D. H. Downie, C. J. Eling, B. K. Charlton, *et al.*, "Recycling self-assembled colloidal quantum dot supraparticle lasers: data," University of Strathclyde, 2024, https://doi.org/10.15129/5825535a-ab05-4678-8102-fe957bdf7943.